ACS APPLIED MATERIALS & INTERFACES

Research Article

www.acsami.org

Gold Nanoparticle-Enabled Blood Test for Early Stage Cancer Detection and Risk Assessment

Tianyu Zheng,[†] Nickisha Pierre-Pierre,[‡] Xin Yan,[§] Qun Huo,*[,†,‡] Alvin J.O. Almodovar,[∥] Felipe Valerio,[∥] Inoel Rivera-Ramirez,[∥] Elizabeth Griffith,[∥] David D. Decker,[∥] Sixue Chen,[⊥] and Ning Zhu[⊥]

[†]NanoScience Technology Center, Department of Chemistry in College of Science, [‡]Burnett School of Biomedical Science in College of Medicine, and [§]Department of Statistics, University of Central Florida, 12424 Research Parkway, Suite 400, Orlando, Florida 32826, United States

[∥]Florida Hospital Cancer Institute, Research and Development, 2501 North Orange Avenue, Suite 247, Orlando, Florida 32804, United States

[⊥]Department of Biology, Genetics Institute, Plant Molecular and Cellular Biology Program, University of Florida, Gainesville, Florida 32610, United States

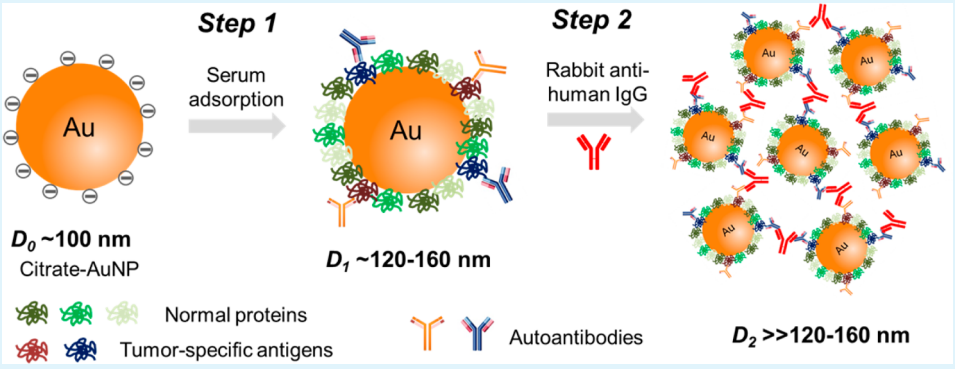

ABSTRACT: When citrate ligands-capped gold nanoparticles are mixed with blood sera, a protein corona is formed on the nanoparticle surface due to the adsorption of various proteins in the blood to the nanoparticles. Using a two-step gold nanoparticle-enabled dynamic light scattering assay, we discovered that the amount of human immunoglobulin G (IgG) in the gold nanoparticle protein corona is increased in prostate cancer patients compared to noncancer controls. Two pilot studies conducted on blood serum samples collected at Florida Hospital and obtained from Prostate Cancer Biorespository Network (PCBN) revealed that the test has a 90−95% specificity and 50% sensitivity in detecting early stage prostate cancer, representing a significant improvement over the current PSA test. The increased amount of human IgG found in the protein corona is believed to be associated with the autoantibodies produced in cancer patients as part of the immunodefense against tumor. Proteomic analysis of the nanoparticle protein corona revealed molecular profile differences between cancer and noncancer serum samples. Autoantibodies and natural antibodies produced in cancer patients in response to tumorigenesis have been found and detected in the blood of many cancer types. The test may be applicable for early detection and risk assessment of a broad spectrum of cancer. This new blood test is simple, low cost, requires only a few drops of blood sample, and the results are obtained within minutes. The test is well suited for screening purpose. More extensive studies are being conducted to further evaluate and validate the clinical potential of the new test.

KEYWORDS: *gold nanoparticle, dynamic light scattering, protein corona, autoantibodies, tumor-specific antigens, cancer detection*

INTRODUCTION

The American Cancer Society estimates that in 2014, there will be approximately 1 665 540 new cancer cases diagnosed and 585 720 cancer deaths in the U.S. Cancer remains the second most common cause of death in the U.S., accounting for nearly 1 of every 4 deaths.[1] Early detection and diagnosis of cancer is critical for effective treatment and reduced mortality. Despite recent advances in molecular diagnostics, noninvasive screening tests for early stage cancer detection are almost nonexistent for most cancer types. The very limited few existing screening tests, such as PSA test for prostate cancer, colonoscopy for colorectal cancer, mammogram for breast cancer, and low dose CT scan for lung cancer either suffer the low specificity and low sensitivity, or involve rather invasive and labor intensive medical procedures, or are too costly to be used for screening purpose.[2] There is a continuing and pressing medical need to develop noninvasive tests for early stage cancer detection and screening.

Received: January 13, 2015
Accepted: March 10, 2015
Published: March 10, 2015

DOI: 10.1021/acsami.5b00371
ACS Appl. Mater. Interfaces 2015, 7, 6819−6827

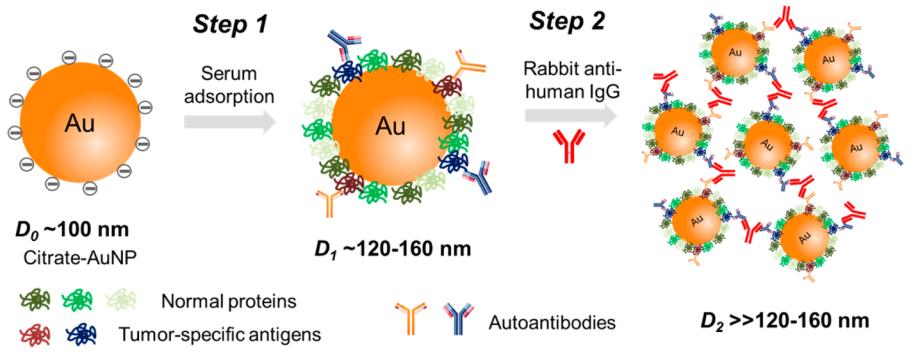

Figure 1. Illustration of a two-step NanoDLSay to analyze the relative amount of human IgG adsorbed to citrate-capped AuNPs for early stage prostate cancer detection. In the first step of the assay, 2 μL of serum is mixed with 40 μL of AuNP solution. Normal blood proteins and tumor-specific antigens from the serum compete to adsorb to the citrate-AuNPs to form a "protein corona". The presence of tumor-specific antigens in the blood serum of cancer patients can cause adsorption of tumor-specific autoantibodies (IgG proteins) to the nanoparticle protein corona. In the second step of the assay, a rabbit antihuman IgG is added to the solution to analyze the relative quantity of human IgG in the adsorbed protein corona. The binding of antihuman IgG with IgG present in the protein corona will lead to nanoparticle cluster formation. The average particle size of the assay solution followed the first step and second step of the assay is measured using dynamic light scattering. The test score is expressed as the ratio of the average particle size of the assay solution obtained from the second (D_2) versus the first step of the assay (D_1), D_2/D_1. Higher ratio corresponds to more IgG present in the protein corona.

Recent advance in nanotechnology has brought many innovative approaches and solutions to biomedical research. Gold nanoparticles (AuNPs) are among one of the most extensively studied and broadly used nanomaterials for biomedical applications.[3−6] AuNPs exhibit exceptionally strong light scattering properties at the surface plasmon wavelength region.[7,8] A AuNP scatters light 100s to 1000 times stronger than a polymer bead at similar size. AuNPs are excellent optical probes for light scattering-based bioimaging and biomolecular detection.[9,10] By combining the strong light scattering property of AuNPs with a technique used routinely for nanoparticle size analysis, dynamic light scattering (DLS), we developed a nanoparticle-enabled dynamic light scattering assay (NanoDLSay) for chemical and biological target analyte detection and analysis.[11,12] NanoDLSay detects target analytes by monitoring the average particle size increase of the AuNP probes upon binding with the target analytes. The binding of target analytes to the AuNP probes either causes individual particle size increase or induces nanoparticle cluster formation. There is a quantitative correlation between the average particle size of the assay solution and the quantity of target analytes in sample solutions. NanoDLSay has so far been applied for quantitative detection and analysis of a wide range of chemical and biological targets, including proteins, DNAs, viruses, carbohydrates, small chemicals, toxic metal ions, food and environmental toxins.[13−20]

Citrate ligand-capped gold nanoparticle (ctAuNP), also called gold colloid, is one of the best known gold nanoparticles.[21,22] Citrate is negatively charged under neutral pH conditions, therefore, ctAuNPs are negatively charged. Because of the unique surface chemistry of ctAuNPs (the negative charge and the hydrophobic Au atoms), proteins tend to adsorb to ctAuNPs through a suite of noncovalent chemical interactions including electrostatic interactions between positively charged amino acid residues and the citrate ligands; van der Waals interactions between hydrophobic moieties of the protein and gold metal core and strong Au−S, Au−N bonding.[23−25] The physical adsorption of antibodies to ctAuNPs is commonly used to prepare gold nanoparticle immunoprobes.[26,27]

Human blood contains thousands of proteins.[28,29] When ctAuNPs are mixed with human blood, studies have shown that both abundant and low abundant blood proteins can adsorb to the nanoparticles to form a "protein corona".[30−32] Because the protein profile in the blood of cancer patients differs from healthy donors, we hypothesize that the molecular composition of the protein corona formed on the ctAuNP surface may differ between cancer and noncancer human blood. While investigating the molecular differences in the protein corona formed on ctAuNPs from prostate cancer and noncancer blood serum samples using NanoDLSay, we discovered in this study that the amount of human immunoglobulin G protein (IgG) in the protein corona is increased in early stage prostate cancer. The increased amount of IgG in the protein corona is believed to be due to the coadsorption of tumor-specific antigens and autoantibodies[33−35] to the AuNPs. The complete procedure of a two-step NanoDLSay used in the present study is illustrated in Figure 1. In the first step of the assay, a small amount of serum sample is directly mixed with a ctAuNP solution. After certain incubation time (5−20 min), the average particle size, D_1, of the mixed solution is measured. Then in a second step of the assay, a rabbit polyclonal antihuman IgG antibody is added to the assay solution to probe the relative amount of human IgG present in the protein corona. When human IgG antibody is present in the protein corona, the binding of rabbit antihuman IgG causes nanoparticle cluster formation due to human IgG and antihuman IgG binding. The nanoparticle cluster formation is detected by measuring the average particle size of the assay solution again (D_2) using DLS following a 5−20 min of incubation time. The more human IgG present in the protein corona, the larger the average particle size increase. The ratio of the average particle size measured in the second step of the assay (D_2) versus the first step of the assay (D_1) is calculated and expressed as the test score to assess the relative quantity of human IgG present in the nanoparticle protein corona.

This test is very easy to perform. Two pilot studies we report here revealed that the new test can discriminate prostate cancer patients from noncancer patients with a 90−95% specificity and 50% sensitivity, a significant improvement over the current PSA test for prostate cancer screening. Because the test detects

DOI: 10.1021/acsami.5b00371
ACS Appl. Mater. Interfaces 2015, 7, 6819−6827

increased immune activities in cancer patients and tumor-specific autoantibodies have been found and detected in a broad spectrum of cancer types,[33] it is possible that this new test may be able to detect other types of cancer as well. More extensive clinical studies are being conducted to further evaluate and validate the potential of this new test as a universal screening test for early stage cancer detection and cancer risk assessment.

RESULTS AND DISCUSSION

Light Scattering Intensity Study of Gold Nanoparticles Mixed with Blood Sera. DLS measures the average particle size of a particle solution by monitoring the scattering light intensity fluctuation coming from all particles in the sample solution.[36] The exceptional light scattering property of AuNP probes is crucial to ensure the successful application of NanoDLSay for biological sample analysis. Biological fluids, such as blood sera contain a large amount of colloidal particles including biomacromolecules (large proteins and polymers), macromolecular complexes, exosomes and vesicles (cell components and fragments), of which the sizes fall in the range between tens and hundreds of nanometers. These biological particles also scatter light intensely. Approximately 40 years ago, Cohen et al. proposed a similar assay concept using polystyrene beads as the light scattering probe and DLS to detect the target analyte binding-induced polystyrene bead cluster formation.[37−39] However, this assay was not pursued actively following its initial publication, presumably because of less-than-expected performance. The light scattering intensity of a polystyrene bead is not significantly stronger than typical biological particles. As a result, the light scattering from the sample matrix contributes significantly to the particle size measurement. For the nanoparticle probe-enabled dynamic light scattering assay to work, the light scattering intensity of the nanoparticle probe must exceed largely the light scattering from the sample matrix, so that the measured average particle size of the assay solution only reflects the particle size change of the nanoparticle probes caused by target analyte binding, but not by the background scattering from the sample matrix.

To experimentally demonstrate the critical importance of a strong light scattering nanoparticle probe in the assay, we examined the light scattering intensity of pure AuNP solution and the effect of the human blood serum on the light scattering of the mixed AuNP-serum assay solution. The light scattering intensity of AuNPs increases with nanoparticle size.[7,8] ctAuNP with two sizes were examined here: 40 nm (AuNP40nm) and 100 nm (AuNP100nm). To prepare the AuNP-serum mixture solution, 2 μL serum was mixed with 40 μL of AuNP solution. This is the serum-AuNP ratio used in the following clinical study. Figure 2 is the intensity-averaged size distribution curves of the two AuNP solutions and their mixtures with a blood serum sample. The two distribution curves of AuNP-serum mixture solutions are representative of multiple serum samples. Before and after the addition of the serum solution, the particle size distribution curves remain relatively monodispersed. The average particle size of AuNP40nm-serum and AuNP100nm-serum increased by about 26 and 20 nm, respectively, compared to the pure AuNP solutions.

Table 1 is a summary of the scattering light intensity study of the four solutions. It first needs to be explicitly pointed out here that the DLS measurements of AuNP40nm and AuNP100nm were conducted using two different incident laser power adjusted by attenuation. The incident laser power used for

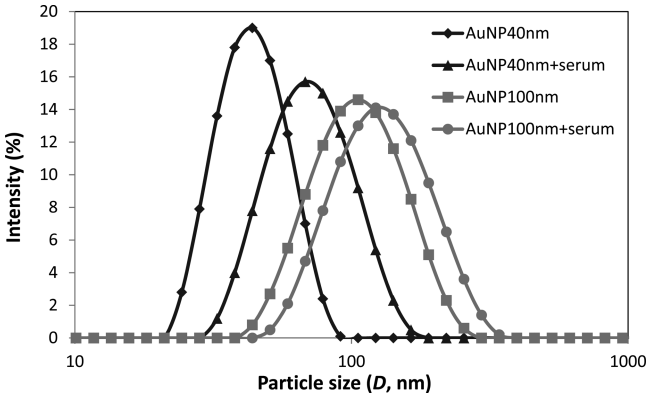

Figure 2. Intensity-averaged size distribution curves of AuNP40nm, AuNP40nm mixed with serum, AuNP100nm, and AuNP100nm mixed with serum. To prepare the mixture of AuNP and serum, 2 μL of serum was added to 40 μL of AuNP solution.

Table 1. Light Scattering Intensity Study of AuNP40nm, AuNP100nm, Serum, and Mixture of Serum with AuNP40nm and AuNP100nm

laser power	scattering light intensity (kcps) ± standard deviation			
	AuNP40nm	serum	serum/ AuNP40nm × 100%	AuNP40nm + serum
attenuation 11	1038 ± 21	509 ± 137	49	1311 ± 24
	AuNP100nm	serum	serum/ AuNP100nm × 100%	AuNP100nm + serum
attenuation 8[a]	1252 ± 30	29 ± 5	2	1239 ± 23

[a]Attenuation 8 decreases the incident laser power to 3% of the laser power at attenuation 11.

AuNP100nm study is approximately 3% of the laser power used for AuNP40nm study. The reason to use less laser power for AuNP100nm study is to avoid potential damage to the detector because of excessive number of photons reaching the detector. The manufacturer recommends to control the photon count rate to be around or less than 1000 kcps (kilo counts per second).[40] Under a 3% laser power, the photon count rate from AuNP100nm solution is at the similar level as AuNP40nm, ∼1000−1200 kcps. In other words, the AuNP100nm solution scatters light approximately 30 times stronger than the AuNP40nm solution. To evaluate the contribution of light scattering from serum to the nanoparticle assay, 2 μL serum was added to 40 μL pure water. Under the 100% and 3% laser power, the photon count rate of this serum control solution is 509 and 29 kcps, respectively. The light scattering intensity from the serum is approximately 49% of the light scattering intensity from AuNP40nm, but only 2% of the light scattering intensity of AuNP100nm. These numbers demonstrate clearly that the AuNP40nm is not suitable for the proposed serum assay, because the background light scattering from the serum will contribute significantly to the average particle size of the assay solution. Indeed, a significant light scattering intensity increase of ∼300 kcps was observed from AuNP40nm solution when serum was added. In contrast, the light scattering intensity from the serum is at the noise level of the AuNP100nm solution. The mixed AuNP100nm-serum solution exhibits almost the same light scattering intensity as the pure

DOI: 10.1021/acsami.5b00371
ACS Appl. Mater. Interfaces 2015, 7, 6819−6827

AuNP100nm solution (1252 versus 1239 kcps). The contribution from the serum particles to particle size measurement of the assay solution can be neglected. Particle size change detected from the AuNP100nm-serum assay solution should arise solely from the AuNP probes. Although only one serum sample is presented here, we have frequently conducted the same analysis on randomly selected serum samples (~10% of the serum sample populations), and the measured light scattering intensity from the serum samples has never exceeded 5% of the light scattering from the AuNP100nm solution. By using AuNP100nm in the serum assay, the background light scattering interference from the serum matrix can be successfully avoided.

AuNP-Serum Adsorption Assay and Adsorbed Human IgG Analysis. Using AuNP100nm as the probe and following a two-step assay format as illustrated in Figure 1, we conducted two pilot studies on prostate cancer and cancer-free human blood serum samples collected at Florida Hospital and obtained from Prostate Cancer Biorespository Network (PCBN). PCBN is a biorepository network that collects, archives and provides human tissue specimens and samples related to prostate cancer through collaboration between the Johns Hopkins University (JHU), the New York University (NYU) School of Medicine, Memorial Sloan Kettering Cancer Center (MSKCC), the University of Washington (UW), and the Department of Defense. The PCBN study was conducted as a blind study, with the patients' clinical information (cancer status and stage) revealed to the researcher after the tests were completed and results were submitted to the network for record keeping. Clinical information on the samples including cancer stage distribution data is summarized in Table 2. More than 80% of cancer cases in both studies are early stage cancer (stage T2a and below). In the first step of the assay, 2 μL serum was mixed with 40 μL AuNP100nm; and in the second step of the assay, a rabbit antihuman IgG antibody solution was added to the AuNP-serum solution to analyze the relative quantity of human IgG adsorbed to the AuNPs. The ratio of the average particle size of the assay solution measured at the second step versus the first step of the assay was expressed as the test score. The detailed procedure of the assay can be found in the corresponding figure captions. The Florida Hospital samples include 32 cancer patients (cancer group) and 23 BPH (benign prostate hyperplasia) patients (BPH group). BPH is a noncancerous prostate condition. The PCBN samples include 20 cancer patients and 19 noncancer controls.

Table 2. Sample Size and Cancer Stage Distribution of Human Serum Samples Used in the Study

sample information			cancer stage distribution				
clinical source	sample group	sample size	HPIN[a], T1a, T1c	T2a	T2b, T2c	T3a	T4
Florida Hospital	cancer	32	22	5	2	3	0
Florida Hospital	BPH	23	N/A				
PCBN	cancer	20	14	2	1	3	0
PCBN	noncancer	19	N/A				

[a]HPIN: High-grade prostatic intraepithelial neoplasia.

There are several slight differences in the protocols used for Florida Hospital study versus PCBN study. The differences between the two sets of protocols are as follows: (1) The incubation time is 6 min for the first step of the assay and 9 min for the second step assay for Florida Hospital study, and the incubation time is 20 min for each step in the PCBN study. (2) The antihuman IgG antibody used in the second step of the assay is ab2410 for Florida Hospital study and ab6715 for PCBN study. All other conditions are the same for both studies. Both ab2410 and ab6715 are rabbit polyclonal antihuman IgG, but ab6715 has a broader binding activity with human IgG than ab2410. As a result of these differences in the assay protocol, the nanoparticle test score expressed as the two-step average particle size ratio D_2/D_1 is larger for the PCBN study compared to the Florida Hospital study. The assay data of these two sets of studies cannot be compared directly with each other. Assay results are presented in Figure 3A (Florida Hospital study) and Figure 3B (PCBN study), respectively. The pairwise p value between sample groups was calculated using ANOVA model and indicated in the graph.

Assay data reveals that a significant number of samples in the cancer groups in both Florida Hospital and PCBN sample set show higher test scores (larger particle size ratio) compared to noncancer groups. From Florida Hospital study, statistical analysis reveals the following: (1) There is a statistically significant test score difference between the cancer group and benign condition BPH group. The p value is 0.001. (2) At a cutoff value of 1.35 (determined by median score of BPH group plus one standard deviation), the test has a 91% specificity and 50% sensitivity in distinguishing benign prostate conditions from cancer. The PCBN study revealed very similar findings as Florida Hospital study: (1) The score difference between cancer and healthy control group is statistically significant (p-value 0.004); (2) At a cutoff value of 2.48 (determined by median score of noncancer group plus two standard deviations), the test has a 95% specificity and 50% sensitivity in distinguishing healthy control from cancer case.

Overall, the test represents a significant improvement over the current PSA test. According to a recent comprehensive review published by the American Cancer Society based on nine major clinical studies conducted around the world, at a cutoff value of 4.0 ng/mL (the most widely adopted clinical cutoff value for PSA test), the PSA test has a 91% specificity and 21% sensitivity.[41] If the PSA cutoff value is decreased to 3.0 ng/mL, the sensitivity of the PSA test is improved to 32%, however, the specificity of the test is decreased to 85%.[41] For the new nanoparticle test, while maintaining a high specificity of 90–95%, the sensitivity of the new test is 50%, more than 2-fold of the PSA test. Another major limiting factor of the current PSA test is its poor specificity in distinguishing early stage prostate cancer from noncancerous benign prostate cancer conditions such as BPH.[42] PSA value in the range of 4–10 ng/mL represents a diagnostic gray zone. In this range, prostate cancer is present in only 25% of the patients.[43] This low specificity (high false positive rate) of PSA test in the diagnostic gray zone is the major cause of overdiagnosis. A study by Stamey et al. showed that most PSA increase up to 9 ng/mL could be attributed to BPH.[44] The fact that the new nanoparticle test can discriminate BPH patients from prostate cancer patients with ~90% specificity is particularly encouraging. The nanoparticle test could potentially be used in combination with the PSA test to significantly improve the specificity of early stage prostate cancer screening and detection, especially in the diagnostic gray zone of PSA value between 4 and 10 ng/mL, reducing the unnecessary overdiagnosis and biopsy procedures performed on men.

DOI: 10.1021/acsami.5b00371
ACS Appl. Mater. Interfaces 2015, 7, 6819–6827

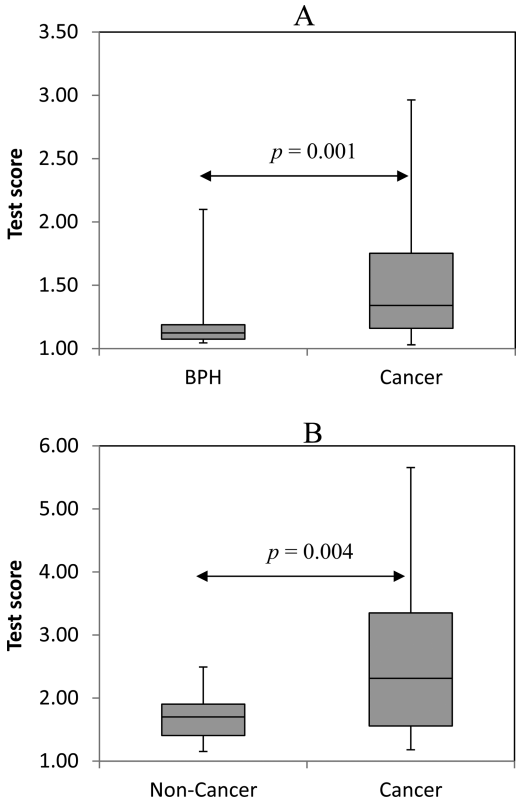

Figure 3. Nanoparticle test results of Florida Hospital (A) and PCBN (B) study. Assay procedure for Florida Hospital study: 2 μL of serum was added to 40 μL of AuNP100nm solution. Following a 6 min of incubation at room temperature, the average particle size (D_1) of the assay solution was measured. Then 2 μL of rabbit antihuman IgG antibody (ab2410) at 2.0 mg/mL was added to the assay solution. Following a 9 min of incubation, the average particle size of the assay solution was measured again (D_2). Assay procedure for PCBN study: 2 μL of serum was added to 40 μL of AuNP100nm solution. Following a 20 min of incubation at room temperature, the average particle size (D_1) of the assay solution was measured. Then 2 μL of rabbit antihuman IgG antibody (ab6715) at 2.4 mg/mL was added to the assay solution. Following a 20 min of incubation, the average particle size of the assay solution was measured again (D_2). For both assays, the test score is expressed as the nanoparticle size ratio of second versus first step assay (D_2/D_1). ANOVA model was used to analyze the statistical difference of group pairs. Pairwise p-values are indicated in the graph. The difference between the group-pairs is considered statistically significant is the p value is of or less than 0.05, and vice versa.

Mechanistic Study of Increased Human IgG in the Nanoparticle Protein Corona Formed in Cancer Patients' Sera. From the first step of the nanoparticle assay, that is, the adsorption of serum proteins to ctAuNPs, the average particle size of the assay solution increased by about 20−60 nm for most serum samples. This indicates no substantial nanoparticle clusters/aggregates were formed from the serum adsorption step. This was expected, because most circulating IgGs are immune-inactive. The AuNP concentration used in the assay is very low, only 10 pM. The small amount of tumor-elicited autoantibodies in the serum is not enough to cause substantial cross-linking of the AuNPs. In the second step of the assay, a rabbit polyclonal anti-IgG was added intentionally in high concentration (2 mg/mL) to the assay solution. This high concentration of anti-IgG drives the cross-linking of AuNPs into aggregates by binding with the small amount of IgG autoantibodies adsorbed to the AuNP surface. We also found the test results expressed as the average nanoparticle size ratio instead of net average nanoparticle increase in the two-step assay can better correlate to cancer status. Therefore, we adopted the average nanoparticle size ratio between the first and the second step of the assay as the test score. Higher test score is interpreted as more human IgGs present on the gold nanoparticle surface. To confirm that the particle size increase observed in the second step of the assay following the addition of rabbit antihuman IgG in the assay solution is indeed caused by specific binding of antihuman IgG with human IgG on the nanoparticle surface, we conducted the same assay using a nonspecific rabbit antibody isotype control. The isotype control caused almost no particle size increase following its addition to the assay solution (Figure 4A).

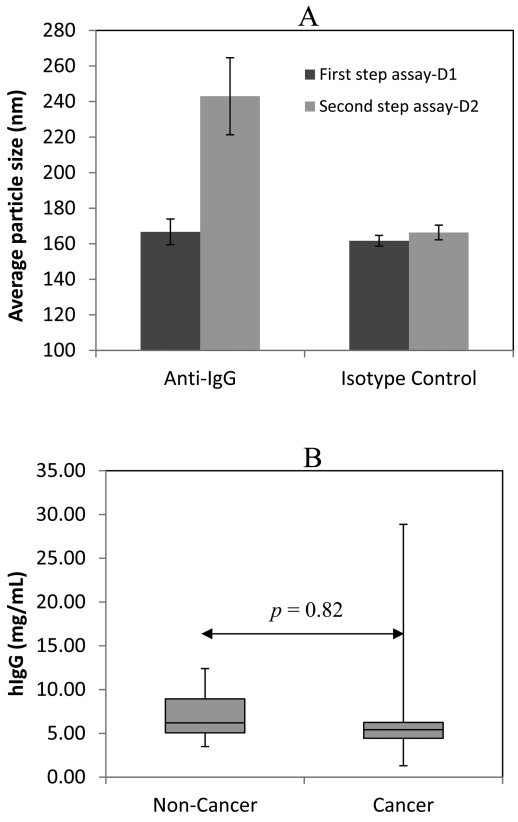

Figure 4. (A) Control study using rabbit IgG isotype control antibody in the two-step nanoparticle test. The first step of the assay is the same as the nanoparticle test as used for PCBN study. In the second step of the assay, a nonspecific rabbit IgG isotype control (ab37415) instead of specific rabbit antihuman IgG was added to the assay solution at the same concentration (2 mg/mL) and same volume (2 μL). (B) ELISA analysis of total quantity of human IgG in PCBN serum sample sets (cancer and noncancer group) using an ELISA kit (ab100547) from Abcam. ANOVA model was used to analyze the p value of cancer and noncancer group pair.

It needs to be emphasized that this nanoparticle test detects only the relative quantity of protein analytes, such as human IgG adsorbed to the AuNPs, not the absolute quantity of human IgG in the blood serum. According to the principal of the assay as discussed earlier, the assay detects only antibody−antigen binding that takes place around the AuNPs, more specifically, around the protein corona formed on the nanoparticle surface. To evaluate if there is a correlation

DOI: 10.1021/acsami.5b00371
ACS Appl. Mater. Interfaces 2015, 7, 6819−6827

between the relative quantity of human IgG present in the AuNP protein corona and the total IgG in the blood serum, we determined the absolute quantity of human IgG antibody in the PCBN sample set using an ELISA kit (ab100547) from Abcam. This assay revealed no significant difference (p-value 0.82) in the total quantity of human IgG between cancer and noncancer group (Figure 4B). There is no correlation between the amount of human IgG in the serum as determined by ELISA and the relative quantity of human IgG in the gold nanoparticle protein corona.

These observations led to an interesting question: why an increased amount of human IgG is present in the nanoparticle protein corona formed in cancer patients' sera while the total quantity of human IgG in the blood sera is about the same for cancer and noncancer group? We hypothesize that the increased amount of human IgG detected in the nanoparticle protein corona of cancer patients' sera is associated with the presence and coadsorption of tumor-specific antigens and autoantibodies (mainly IgG proteins)[33−35] to the AuNPs. According to cancer immunoediting theory,[45,46] the host immune system can recognize transformed tumor cells as nonself, and will trigger certain immune defensive responses to prevent primary tumor growth. Autoantibodies or natural antibodies against tumor-specific antigens have been detected widely in many cancer types and are being actively pursued as potential biomarkers for early stage cancer detection.[33−35,47−54] Using a phage display and protein microarray technique, Wang et al. identified a 22 phage-displayed peptide panel that detects autoantibody signatures in the blood of prostate cancer patients.[34] Xie et al. developed a multiplex assay combining the detection of six autoantibodies associated with prostate tumor and PSA, and the assay provides both enhanced sensitivity and specificity for prostate cancer detection compared to PSA test alone.[35] In the nanoparticle test, tumor-released antigens compete with other serum proteins to adsorb to the citrate-AuNPs. The AuNP functions as a "mini-concentrator" to attract both normal blood proteins and tumor-specific antigens to the nanoparticle surface. Subsequently, autoantibodies that are specific to these tumor-associated antigens are coadsorbed to the AuNPs by binding with the adsorbed tumor antigens, as illustrated in Figure 1. As a result, an increased amount of IgG proteins was detected in the nanoparticle protein corona formed from cancer patients' sera. This phenomenon was previously observed from a limited study we conducted on mouse models carrying prostate tumor.[55]

To support our hypothesis, we conducted proteomic analysis on the proteins adsorbed to the AuNPs from several cancer and noncancer serum samples. After the serum sample was mixed with AuNP solution for 2 h at rt, the serum-adsorbed AuNP product was isolated and purified by centrifuge followed by washing with phosphate buffer solution twice. The adsorbed proteins were released from the AuNPs by trypsin digestion and then analyzed using a LTQ-Orbitrap mass spectrometer and method as previously described,[56] except the database used for protein searching was the human protein database. Table 3 listed two groups of proteins that are either absent in the cancer sera but present in the normal sera; or are present in the cancer sera but absent in the normal serum. This short list illustrates that the molecular profile of the protein corona adsorbed to the AuNPs indeed differs between cancer and noncancer sera. Some of the proteins that were found in cancer sera but not in normal control sera are potentially tumor-associated antigens and these antigens attracted their autoantibodies to the nanoparticle surface, leading to an increased amount of IgG protein in the protein corona. More extensive studies need to be conducted to elucidate the identities of the tumor antigens adsorbed to the ctAuNPs and such antigens may serve as biomarkers for specific cancer detection.

Table 3. List of Selected Proteins and Peptides That Differ in the Gold Nanoparticle Protein Coronas Formed in Prostate Cancer and Non-cancer Blood Sera[a]

protein identity	normalized total spectrum count: cfu5 (T3a cancer)	cfu40 (T3a cancer)	cfu17 (noncancer)
proteins that are absent in cancer serum but present in normal serum			
cluster of 13 kDa protein	0	0	6
13 kDa protein	0	0	5
13 kDa protein	0	0	6
cluster of antistreptococcal/antimyosin immunoglobulin lambda light chain variable region	0	0	53
putative uncharacterized protein			
cluster of cold agglutinin FS-1 L-chain			
13 kDa protein	0	0	5
cluster of Ig kappa chain V−III region			
HRV Fab N27-VL	0	0	10
cluster of uncharacterized protein			
HRV Fab 025-VL	0	0	7
cluster of VH6DJ protein			
VH6DJ protein	0	0	6
hemoglobin subunit alpha	0	0	5
proteins that are present in cancer serum but absent in normal serum			
cluster of antistreptococcal/antimyosin immunoglobulin lambda light chain variable region			
Ig lambda chain V−I region VOR	6	3	0
cluster of cold agglutinin FS-1 L-chain			
cold agglutinin FS-1 L-chain	5	4	0
Ig kappa chain V−I region CAR	11	7	0
isoform 3 of keratin, type I cytoskeletal 13	25	26	0
cluster of hypothetical protein LOC100291917	18	9	0
Ig heavy chain V−II region SESS	5	3	0
hypothetical protein LOC100291917	17	8	0

[a]Selection criteria: the normalized total spectrum count of the protein/peptide is at least 5 or above.

CONCLUSION

Tumor antigen-specific autoantibodies are known to appear months even years before clinical diagnosis of cancer, and autoantibodies have been found in many types of cancer.[43−50] Autoantibodies are excellent biomarkers for early stage cancer detection and screening. According to cancer immunoediting theory,[45,46] the host immunodefense activity against tumor occurs at early stage of tumor development. At later stages, tumor may develop the capability to "escape" the immunosurveillance.[45,46] This hints that there is an optimum time window to detect the increased immune activity in cancer patients. If the new nanoparticle test is applied as an annual screening test, the sensitivity of the test could potentially increase from the current 50% to a much higher level. Most studies are attempting to identify tumor-specific antigens, and detect antibodies that are specific to individual tumor-

DOI: 10.1021/acsami.5b00371
ACS Appl. Mater. Interfaces 2015, 7, 6819−6827

associated antigens. Different from these approaches, the nanoparticle test we report here detects an overall increase of human IgG (including the tumor-specific autoantibodies) adsorbed to a AuNP surface. On one hand, this test may not be able to identify the specific type of cancer; on the other hand, this test may potentially be able to detect early stage tumor-induced immune responses associated with a broad spectrum of cancer types, making this test potentially a universal screening test for cancer risk assessment. The new test may be combined with other cancer type-specific test such as PSA test for prostate cancer to improve the early detection and diagnosis of specific cancer types. More extensive clinical studies are being pursued to further validate the clinical applications of the new nanoparticle test, and to evaluate comprehensively the potential interference of other medical conditions and clinical factors that may affect the specificity and sensitivity of the test.

In summary, we reported here a unique nanoparticle-enabled blood test with clinical potential for early stage cancer screening and detection. The test successfully utilizes the exceptional light scattering property of gold nanoparticles for target protein detection. The test is extremely simple, of low cost, requires a few drops of blood samples that can be collected from a finger prick instead of a blood draw, and may be conducted in a point-of-care facility such as a doctor's office. The test is well suited for screening purpose.

EXPERIMENTAL PROCEDURES

Chemical and Biochemical Reagents. Citrate-protected gold nanoparticles, AuNP40nm (15707−1, conc. 9.0×10^{10} particles/mL) and AuNP100nm (15708−9, conc. 5.6×10^{9} particles/mL), were purchased from Ted Pella, Inc. (Redding, CA). Rabbit polyclonal antihuman IgG (ab2410 and ab6715), rabbit IgG isotype control (ab37415), and ELISA kit (ab100547) for human IgG analysis of blood serum samples were purchased from Abcam (Cambridge, MA).

Dynamic Light Scattering (DLS) Analysis. The scattering light intensity study of AuNPs and AuNP-serum mixture solutions was conducted using a Zetasizer Nano ZS90 DLS system equipped with a green (532 nm, 4 mW) laser and an Avalanche photodiode detector (APD) (quantum efficiency >50% at 532 nm) (Malvern Instruments Ltd., England). The incident laser power can be adjusted by using different attenuations. All AuNP-serum assays were conducted using an automatic NDS1200 DLS instrument from Nano Discovery Inc. (Orlando, FL). This system is equipped with a 633 nm He−Ne laser (0.5 mW) and a 12-sample holder, which allow measurement of 12 samples within 6 min. All size measurements were conducted at an ambient temperature of 25 °C.

Serum-AuNP Adsorption Assay and the Adsorbed Human IgG Analysis. To perform the serum-AuNP adsorption assay and the human IgG analysis, 2 μL of serum was mixed with 40 μL of AuNP100nm. After incubating for 5−20 min, the average particle size of the assay solution (D_1) was measured using NDS1200. Then 2 μL of rabbit antihuman IgG (2 mg/mL) was added to the assay solution. After it was incubated for another 5−20 min, the average particle size of the assay solution (D_2) was measured again. The ratio of D_2/D_1 was calculated as the test score. Specific assay incubation time can be found in the corresponding figure captions. Statistical analysis of the assay data was conducted to calculate the group pair p-value using ANOVA (Analysis of Variance) model.

Human Subject Research and Protection. The Florida Hospital study was reviewed and approved by both Institutional Review Board committees at University of Central Florida and Florida Hospital (IRB approval number: 288679-4). The study using PCBN samples was reviewed and approved by University of Central Florida. For Florida Hospital study, informed consent was obtained from all participants and study protocol was strictly followed during the study. No problems or harm to the participants were encountered or noticed during the study.

Blood samples were collected using Serum Separator Tube (SST). Immediately after obtaining the blood sample, the tube was inverted 5 to 6 times. The tube was placed in an upright position for 30 min to allow complete blood clotting. Tubes were not refrigerated or opened during this process. The SST contains a special gel at the bottom of the tube that migrate during centrifugation and separate cells and serum at the end of the centrifugation process. The tube was centrifuged within the next 30 min (within 1 h from collection) for 10 min at 1500g.

The study using archived, deidentified blood serum samples from PCBN was determined as "Not Human Subject Research" as defined by DHHS regulations at 45 CFR 46 or FDA regulations at 21 CFR 50/56. Total 20 prostate cancer samples and 20 normal control samples were received from PCBN. One normal sample was rejected as an extreme outlier in the statistics analysis: the test score of this sample was 6.43, largely exceeding the upper outer fence value of 3.4 of the normal control group.

Proteomic Analysis of Gold Nanoparticle Protein Corona. To prepare the sample for proteomic analysis, AuNP100nm was first concentrated 10 times from 1 mL to 100 μL by centrifuge. Then to 400 μL of 10× concentrated AuNP100nm, 2 μL of serum was added. After incubating at r.t. for 2 h, the solution was centrifuged at 5 kilo rmp using an Eppendorf minispin centrifuge for 3 min. After removing the suspension, the nanoparticle residues were washed twice with 10 mM phosphate buffer solution. After decanting the second phosphate buffer washing solution, the samples were ready for trypsin digestion. Three serum samples were prepared for proteomic analysis: two cancer serum samples (cfu5 and cfu40, both from T3a prostate cancer patients), and one noncancer healthy control (cfu17). The trypsin digest was loaded onto a nanoflow HPLC-LTQ Orbitrap mass spectrometer system (Thermo Scientific Inc., Bremen, Germany) and the data were analyzed as described previously described.[56] The database used was IPI human with 91 464 entries.

AUTHOR INFORMATION

Corresponding Author

*E-mail: Qun.Huo@ucf.edu. Tel: 407-882-2845.

Notes

The authors declare the following competing financial interest(s): Q. Huo is an owner and officer of Nano Discovery Inc. This company may be interested in commercializing the new blood test for cancer detection.

ACKNOWLEDGMENTS

This work is supported by the Department of Defense Prostate Cancer Research Program, DOD Award No W81XWH-10-2-0056 and W81XWH-10-2-0046 PCRP Prostate Cancer Biorepository Network (PCBN). We also thank Prof. Bruce Trock from Johns Hopkins University for his collaboration and suggestions in the study of PCBN specimens.

REFERENCES

(1) Statistics from the American Cancer Society. www.cancer.org.

(2) Smith, R. A.; Manassaram-Baptiste, D.; Brooks, D.; Cokkinides, V.; Doroshenk, M.; Saslow, D.; Wender, R. C.; Brawley, O. W. Cancer Screening in the United States, 2014: A Review of Current American Cancer Society Guidelines and Issues in Cancer Screening. *Ca—Cancer J. Clin.* **2014**, *64*, 30−51.

(3) Jans, H.; Huo, Q. Gold Nanoparticle-Enabled Biological and Chemical Detection and Analysis. *Chem. Soc. Rev.* **2012**, *41*, 2849−2866.

(4) Dykman, L.; Khlebtsov, N. Gold Nanoparticles in Biomedical Applications: Recent Advances and Perspectives. *Chem. Soc. Rev.* **2012**, *41*, 2256−2282.

DOI: 10.1021/acsami.5b00371
ACS Appl. Mater. Interfaces 2015, 7, 6819−6827

(5) Dreaden, E. C.; Alkilany, A. K.; Huang, X.; Murphy, C. J.; El-Sayed, M. A. The Golden Age: Gold Nanoparticles for Biomedicine. *Chem. Soc. Rev.* **2012**, *41*, 2740−2779.
(6) Saha, K.; Agasti, S. S.; Kim, C.; Li, Rotello, V. M. Gold Nanoparticles in Chemical and Biological Sensing. *Chem. Rev.* **2012**, *112*, 2739−2779.
(7) Yguerabide, J.; Yguerabide, E. E. Light-Scattering Submicroscopic Particles as Highly Fluorescent Analogs and Their Use as Tracer Labels in Clinical and Biological Applications. *Anal. Biochem.* **1998**, *262*, 137−156.
(8) Jain, P. K.; Lee, K. S.; El-Sayed, I. H.; El-Sayed, M. A. Calculated Absorption and Scattering Properties of Gold Nanoparticles of Different Size, Shape, and Composition: Applications in Biological Imaging and Biomedicine. *J. Phys. Chem. B* **2006**, *110*, 7238−7248.
(9) El-Sayed, I. H.; Huang, X.; El-Sayed, M. A. Surface Plasmon Resonance Scattering and Absorption of Anti-EGFR Antibody Conjugated Gold Nanoparticles in Cancer Diagnostics: Applications in Oral Cancer. *Nano Lett.* **2005**, *5*, 829−834.
(10) Kang, B.; Austin, L. A.; El-Sayed, M. A. Observing Real-Time Molecular Event Dynamics of Apoptosis in Living Cancer Cells Using Nuclear-Targeted Plasmonically Enhanced Raman Nanoprobes. *ACS Nano* **2014**, *8*, 4883−3892.
(11) Liu, X.; Dai, Q.; Austin, L.; Coutts, J.; Knowles, G.; Zou, J.; Chen, H.; Huo, Q. A One-Step Homogeneous Immunoassay for Cancer Biomarker Detection Using Gold Nanoparticle Probes Coupled with Dynamic Light Scattering. *J. Am. Chem. Soc.* **2008**, *130*, 2780−2782.
(12) Dai, Q.; Liu, X.; Coutts, J.; Austin, L.; Huo, Q. A One-Step Highly Sensitive Method for DNA Detection Using Dynamic Light Scattering. *J. Am. Chem. Soc.* **2008**, *130*, 8138−8139.
(13) Kalluri, J. R.; Arbneshi, T.; Afrin Khan, S.; Nelly, A.; Candice, P.; Varisli, B.; Washington, M.; McAfee, S.; Robinson, B.; Banerjee, S.; Singh, A. K.; Senapati, D.; Ray, P. C. Use of Gold Nanoparticles in a Simple Colorimetric and Ultrasensitive Dynamic Light Scattering Assay: Selective Detection of Arsenic in Groundwater. *Angew. Chem., Int. Ed.* **2009**, *48*, 9668−9671.
(14) Driskell, J. D.; Jones, C. A.; Tompkins, S. M.; Tripp, R. A. One-Step Assay for Detecting Influenza Virus Using Dynamic Light Scattering and Gold Nanoparticles. *Analyst* **2011**, *136*, 3083−3090.
(15) Jans, H.; Liu, X.; Austin, L.; Maes, G.; Huo, Q. Dynamic Light Scattering as a Powerful Tool for Gold Nanoparticle Bioconjugation and Biomolecular Binding Study. *Anal. Chem.* **2009**, *81*, 9425−9432.
(16) Wang, X.; Ramström, O.; Yan, M. Dynamic Light Scattering as an Efficient Tool to Study Glyconanoparticle-Lectin Interactions. *Analyst* **2011**, *136*, 4174−4178.
(17) Wang, L.; Zhu, Y.; Xu, L.; Chen, W.; Kuang, H.; Liu, L.; Agarwal, A.; Xu, C.; Kotov, N. A. Side-by-Side and End-to-End Gold Nanorod Assemblies for Environmental Toxin Sensing. *Angew. Chem., Int. Ed.* **2010**, *49*, 5472−5475.
(18) Wang, X.; Li, Y.; Quan, D.; Wang, J.; Zhang, Y.; Du, J.; Peng, J.; Fu, Q.; Zhou, Y.; Jia, S.; Wang, Y.; Zhan, L. Detection of Hepatitis B Surface Antigen by Target-Induced Aggregation Monitored by Dynamic Light Scattering. *Anal. Biochem.* **2012**, *428*, 119−125.
(19) Yin, H.; Huang, X.; Ma, W.; Xu, L.; Zhu, S.; Kuang, H.; Xu, C. Ligation Chain Reaction Based Gold Nanoparticle Assembly for Ultrasensitive DNA Detection. *Biosens. Bioelectron.* **2014**, *52*, 8−12.
(20) Zhang, Z.; Lin, M.; Zhang, S.; Vardhanabhuti, B. Detection of Aflatoxin M1 in Milk by Dynamic Light Scattering Coupled with Superparamagnetic Beads and Gold Nanoprobes. *J. Agric. Food Chem.* **2013**, *61*, 4520−4525.
(21) Turkevich, J.; Stevenson, P. C.; Hillier, J. A Study of the Nucleation and Growth Processes in the Synthesis of Colloidal Gold. *Discuss. Faraday Soc.* **1951**, *11*, 55−75.
(22) Kimling, J.; Maier, M.; Okenve, B.; Kotaidis, V.; Ballot, H.; Plech, A. Turkevich Method for Gold Nanoparticle Synthesis Revisited. *J. Phys. Chem. B* **2006**, *110*, 15700−15707.
(23) Calzolai, L.; Franchini, F.; Gilliland, D.; Rossi, F. Protein−Nanoparticle Interaction: Identification of the Ubiquitin−Gold Nanoparticle Interaction Site. *Nano Lett.* **2010**, *10*, 3101−3105.
(24) Brewer, S. H.; Glomm, W. R.; Johnson, M. C.; Knag, M. K.; Franzen, S. Probing BSA Binding to Citrate-Coated Gold Nanoparticles and Surfaces. *Langmuir* **2005**, *21*, 9303−9307.
(25) Glomm, W. R.; Halskau, Ø.; Hanneseth, A.-M. D.; Volden, S. Adsorption Behavior of Acidic and Basic Proteins onto Citrate-Coated Au Surfaces Correlated to Their Native Fold, Stability, and PI. *J. Phys. Chem. B* **2007**, *111*, 14329−14345.
(26) De Mey, J. Colloid Gold Probes in Immunocytochemistry. In *Immunocytochemistry—Practical Applications in Pathology and Biology*, Polak, J. M., Van Norden, D., Eds., Wright: Bristol, England, 1983.
(27) Hermanson, G. T. *Bioconjugate Techniques*, 2nd ed.; Pierce Biotechnology, Thermo Fisher Scientific: Rockford, 2008; Chapter 24.
(28) Krebs, H. Chemical Composition of Blood Plasma and Serum. *Annu. Rev. Biochem.* **1950**, *19*, 409−430.
(29) Anderson, N. L.; Polanski, M.; Pieper, R.; Gatlin, T.; Tirumalai, R. S.; Conrads, T. P.; Veenstra, T. D.; Adkins, J. N.; Pounds, J. G.; Fagan, R. The Human Plasma Proteome a Nonredundant List Developed by Combination of Four Separate Sources. *Mol. Cell. Proteomics* **2004**, *3*, 311−326.
(30) Dobrovolskaia, M. A.; Patri, A. K.; Zheng, J.; Clogston, J. D.; Ayub, N.; Aggarwal, P.; Neun, B. W.; Hall, J. B.; McNeil, S. E. Interaction of Colloidal Gold Nanoparticles with Human Blood: Effects on Particle Size and Analysis of Plasma Protein Binding Profiles. *Nanomedicine* **2009**, *5*, 106−117.
(31) Lacerda, S. H. D. P.; Park, J. J.; Meuse, C.; Pristinski, D.; Becker, M. L.; Karim, A.; Douglas, J. F. Interaction of Gold Nanoparticles with Common Human Blood Proteins. *ACS Nano* **2010**, *4*, 365−379.
(32) Zhang, S.; Moustafa, Y.; Huo, Q. Different Interaction Modes of Biomolecules with Citrate-Capped Gold Nanoparticles. *ACS Appl. Mater. Interfaces* **2014**, *5*, 21184−21192.
(33) Zaenker, P.; Ziman, M. R. Serologic Autoantibodies as Diagnostic Cancer Biomarkers—A Review. *Cancer Epidemiol., Biomarkers Prev.* **2013**, *22*, 2161−2181.
(34) Wang, X.; Yu, J.; Sreekumar, A.; Varambally, S.; Shen, R.; Giacherio, D.; Mehra, R.; Montie, J. E.; Pienta, K. J.; Sanda, M. G.; Kantoff, P. W.; Rubin, M. A.; Wei, J. T.; Ghosh, D.; Chinnaiyan, A. M. Autoantibody Signatures in Prostate Cancer. *N. Engl. J. Med.* **2005**, *353*, 1224−1235.
(35) Xie, C.; Kim, H. J.; Haw, J. G.; Kalbasi, A.; Gardner, B. K.; Li, G.; Rao, J.; Chia, D.; Liong, M.; Punzalan, R. R.; Marks, L. S.; Pantuck, A. J.; de la Taille, A.; Wang, G.; Mukouyama, H.; Zeng, G. A Novel Multiplex Assay Combining Autoantibodies Plus PSA Has Potential Implications for Classification of Prostate Cancer from Nonmalignant Cases. *J. Transl. Med.* **2011**, *9*, 43.
(36) Berne, B. J.; Pecora, R. *Dynamic Light Scattering: With Applications to Chemistry, Biology and Physics*; John Wiley & Sons: New York, 1976.
(37) Cohen, R. J.; Benedek, G. B. Immunoassay by Light Scattering Spectroscopy. *Immunochemistry* **1975**, *12*, 963−966.
(38) Von Schulthess, G. K.; Cohen, R. J. Laser Light Scattering Spectroscopic Immunoassay for Mouse IgA. *Immunochemistry* **1976**, *13*, 955−962.
(39) Von Schulthess, G. K.; Cohen, R. J.; Benedek, G. B. Laser Light Scattering Spectroscopic Immunoassay in the Agglutination-Inhibition Mode for Human Chorionic Gonadotropin (hCG) and Human Luteinizing Hormone (hLH). *Immunochemistry* **1976**, *13*, 963−966.
(40) The User Manual from Malvern Instruments on ZS90 DLS system.
(41) Wolf, A. M. D.; Wender, R. C.; Etzioni, R. B.; Thompson, I. M.; D'Amico, A. V.; Volk, R. J.; Brooks, D. D.; Dash, C.; Guessous, I.; Andrews, K.; DeSantis, C.; Smith, R. A. American Cancer Society Guideline for the Early Detection of Prostate Cancer Update 2010. *Ca—Cancer J. Clin.* **2010**, *60*, 70−98.
(42) Meigs, J. B.; Barry, M. J.; Oesterling, J. E.; Jaconson, S. J. Interpreting Results of Prostate-Specific Antigen Testing for Early Detection of Prostate Cancer. *J. Gen. Int. Med.* **1996**, *11*, 505−512.
(43) Catalona, W. J.; Richie, J. P.; Ahmann, F. R.; Hudson, M. A.; Scardino, P. T.; Flanigan, R. C.; deKernion, J. B.; Ratliff, T. L.; Kavoussi, L. R.; Dalkin, B. L. Comparison of Digital Rectal

DOI: 10.1021/acsami.5b00371
ACS Appl. Mater. Interfaces 2015, 7, 6819−6827

Examination and Serum Prostate Specific Antigen in the Early Detection of Prostate Cancer: Results of a Multicenter Clinical Trial of 6630 men. *J. Urol.* **1994**, *151*, 1283−1290.
(44) Stamey, T. A.; Johnstone, I. M.; McNeal, J. E.; Lu, A. Y.; Yemoto, C. M. Preoperative Serum Prostate Specific Antigen Levels Between 2 and 22 ng/mL Correlate Poorly With Post-Radical Prostatectomy Cancer Morphology: Prostate Specific Antigen Cure Rates Appear Constant Between 2 and 9 ng/mL. *J. Urol.* **2002**, *167*, 103−111.
(45) Dunn, G. P.; Bruce, A. T.; Ikeda, H.; Old, L. J.; Schreiber, R. D. Cancer Immunoediting: From Immunosurveillance to Tumor Escape. *Nat. Immunol.* **2002**, *3*, 991−998.
(46) Dunn, G. P.; Old, L. J.; Schreiber, R. D. The Three Es of Cancer Immunoediting. *Annu. Rev. Immunol.* **2004**, *22*, 329−360.
(47) Lacombe, J.; Mangé, A.; Solassol, J. Use of Autoantibodies to Detect the Onset of Breast Cancer. *J. Immunol. Res.* **2014**, No. 574981.
(48) Wandall, H. H.; Blixt, O.; Tarp, M. A.; Pedersen, J. W.; Bennett, E. P.; Mandel, U.; Ragupathi, G.; Livingston, P. O.; Hollingswoth, M. A.; Taylor-Papadimitriou, J.; Burchell, J.; Clausen, H. Cancer Biomarkers Defined by Autoantibody Signatures to Aberrant O-Glycopeptide Epitopes. *Cancer Res.* **2010**, *70*, 1306−1313.
(49) Kazarian, M.; Laird-Offringa, A. Small-Cell Lung Cancer-Associated Autoantibodies: Potential Applications to Cancer Diagnosis, Early Detection, and Therapy. *Mol. Cancer* **2011**, *10*, 33.
(50) Woodard, K. M.; Chapman, C. J. Lung Cancer-Can Autoantibodies Provide an Aid to Diagnosis? *Expert Opin. Med. Diagn.* **2008**, *2*, 911−923.
(51) Díaz-Zaragoza, M.; Hernández, R.; Ostoa-Saloma, P. 2D Immunoblots Show Differential Response of Mouse IgG and IgM Antibodies to Antigens of Mammary Carcinoma 4 T1 Cells. *Cancer Cell Int.* **2014**, *14*, 9.
(52) Caron, M.; Choquet-Kastylevsky, G.; Joubert-Caron, R. Cancer Immunomics Using Autoantibody Signatures for Biomarker Discovery. *Mol. Cell. Proteomics* **2007**, *6*, 1115−1122.
(53) Brändlein, S.; Pohle, T.; Ruoff, N.; Wozniak, E.; Müller-Hermelink, H.-K.; Vollmers, H. P. Natural IgM Antibodies and Immunosurveillance Mechanisms Against Epithelial Cancer Cells in Humans. *Cancer Res.* **2003**, *63*, 7995−8005.
(54) Vollmers, H. P.; Brändlein, S. Natural Antibodies and Cancer. *J. Autoimmun.* **2007**, *29*, 295−302.
(55) Huo, Q.; Colon, J.; Cordero, A.; Bogdanovic, J.; Baker, C. H.; Goodison, S.; Pensky, M. Y. A Facile Nanoparticle Immunoassay for Cancer Biomarker Discovery. *J. Nanobiotechnol.* **2011**, *9*, 20.
(56) Silva-Sanchez, C.; Chen, S.; Li, J.; Chourey, P. S. A Comparative Glycoproteome Study of Transfer Cells-Enriched Basal Endosperm in the Hexose-Deficient Miniature1 (mn1) Seed Mutant and Its Wild Type Mn1 in Maize. *Front. Plant Sci.* **2014**, *5*, 63.

DOI: 10.1021/acsami.5b00371
ACS Appl. Mater. Interfaces 2015, 7, 6819−6827